Interaction and Multiscale Mechanics, Vol. 3, No. 2 (2010) 173-191
DOI: http://dx.doi.org/10.12989/imm.2010.3.2.173

The tap-scan method for damage detection of bridge structures

Zhihai Xiang*, Xiaowei Dai, Yao Zhang and Qiuhai Lu

Applied Mechanics Laboratory, Department of Engineering Mechanics, Tsinghua University, Beijing, 100084, P. R. China

(Received November 20, 2009, Accepted January 20, 2010)

Abstract. Damage detection plays a very important role to the maintenance of bridge structures. Traditional damage detection methods are usually based on structural dynamic properties, which are acquired from pre-installed sensors on the bridge. This is not only time-consuming and costly, but also suffers from poor sensitivity to damage if only natural frequencies and mode shapes are concerned in a noisy environment. Recently, the idea of using the dynamic responses of a passing vehicle shows a convenient and economical way for damage detection of bridge structures. Inspired by this new idea and the well-established tap test in the field of non-destructive testing, this paper proposes a new method for obtaining the damage information through the acceleration of a passing vehicle enhanced by a tapping device. Since no *finger-print* is required of the intact structure, this method can be easily implemented in practice. The logistics of this method is illustrated by a vehicle-bridge interaction model, along with the sensitivity analysis presented in detail. The validity of the method is proved by some numerical examples, and remarks are given concerning the potential implementation of the method as well as the directions for future research.

Keywords: bridge; damage; non-destructive testing; sensitivity; tap-scan method; vehicle.

1. Introduction

The early alert of damage existence in bridge structures is crucial to bridge maintenance and prognosis. Existing damage detection methods are usually based on the structural dynamic properties, such as natural frequencies and mode shapes (Farrar *et al*. 2001, Carden and Fanning 2004). In conventional vibration tests, the pre-installed measurement instruments record the bridge responses under either the operating loadings, such as the impact from a shaker or a truck, or the environmental loadings, such as wind or traffic flows. The sensor installation and the testing procedure are usually very time-consuming and costly. Besides, the operating loadings can be problematic, in that they are usually strong enough to activate the damage, not to mention that they may also require the traffic to be blocked. Although the environmental loadings do not interrupt the normal operation of the bridge, they can be too weak to excite the responses containing the damage information. Furthermore, even if these properties are accurately obtained, they may not be sensitive

* Corresponding author, Professor, E-mail: xiangzhihai@tsinghua.edu.cn

to damage if only global information is involved, since damage is a local phenomenon (Xiang and Zhang 2009).

Instead of mounting sensors on the bridge, the idea of using a single sensor to scan the bridge leads to a convenient and economical technique for obtaining the dynamic responses. Yang *et al*. (2004) proposed a new concept of extracting bridge frequencies from a passing vehicle. They gave a detailed analysis of this vehicle-bridge interaction problem and discussed some influential factors to the success of this method. Later on, they did conduct an experiment on a real highway bridge to illustrate how to extract the fundamental frequency of that bridge through a passing vehicle (Lin and Yang 2005) and kept on modifying this method by adopting the empirical mode decomposition method for signal processing (Yang and Chang 2009a) and by analyzing the impact of some amplitude ratios to the success of identifying the bridge frequencies (Yang and Chang 2009b). Inspired by the idea of Yang, Bu *et al*. (2006) proposed an inverse approach to identify the damage index, the change of bridge elemental stiffness, from the dynamic response of a vehicle moving over the bridge. They discussed two vehicle models and the influence of road surface roughness. A moving oscillator was used as an excitation source in the damage detection study by Majumder and Manohar (2003, 2004), which require the vibrations of both the vehicle and bridge to be measured. Based on numerical simulations, discussions were also given on the nonlinear effects and spatial incompleteness of the measurement.

Although the aforementioned methods showed some potential for damage detection in a convenient manner, in practice the passing vehicle alone may not excite structural responses that contain enough damage information. It seems that additional excitation is needed to enhance the sensitivity to damage. On the other hand, one may recall that there is actually a very old technology of non-destructive testing, i.e., the tap test. For example, many inspectors use small hammers tapping around the floor to check whether the brick is firmly attached to the ground. It is known that flawed regions sound 'dead' and therefore can be identified. In the similar way, the coin-tap test has been widely used to detect damages in thin-walled aerospace structures for many years. The same phenomenon also exists in the nature. For example, woodpeckers can detect the worm under the bark by tapping the trunk with its beak. Although the tap test has existed for many years, the first attempt to give a rigorous explanation of its mechanics dates back to the work of Cawley and Adams (1988). They conceived that the difference in the sounds produced when good and flawed regions are tapped is due to a change in the impact force. If the same hammer is dropped from the same height, the impact force is only determined by the local impedance of the structure, which changes with the existence of damage. Based on their theory, some digitalized hammers are designed, which can record the time history of impact force. Either the duration of the impact force or the area information of the force spectrum are compared with intact ones, in such a way the damage can be identified. The sensitivity study showed that the defects of 10 mm in diameter can be reliably detected under 1 mm thick composite skins by this method (Cawley and Adams 1989).

Inspired by the passing vehicle test method and the tap test, this paper proposes a tap-scan method that identifies the bridge damage through the acceleration of a passing vehicle mounted with a tapping device. Because the tapping force and vehicle suspension system can be designed for a specific bridge, the acceleration of the vehicle can be rather sensitive to damage in a noisy environment. With this method, the acceleration signal is equally divided into small segments, and time-frequency analysis is carried out for each segment to get the corresponding power spectrum. Because the contour of the power spectrum can be regarded as the feature of the effective impedance of a segment and because the local impedance usually changes smoothly over an intact

structure, damage can be identified by an abrupt change of the power spectrum contour via the Modal Assurance Criterion (MAC). This means that the *finger-print* of the intact structure is not needed in this damage detection method, which can greatly facilitate its practical implementation.

The following text is organized as follows: Section 2 presents the theoretical formulation of the tap-scan damage detection method together with the sensitivity analysis. Section 3 gives some numerical examples to validate this method and shows the potential of its damage detection ability. Section 4 is a conclusion part, in which the direction for future research is also pointed out.

2. Theory of the tap-scan method

As shown in Fig. 1, a simplified model is adopted to illustrate the theoretical basis of the proposed tap-scan method. In this model, the vehicle is modeled as a mass M supported on a spring of stiffness k_V and mounted with two opposite, eccentric wheels $\overline{m}r$ rotating at constant angular speed $\overline{\omega}_i$ (i = 1, 2, …, N) each from the initial angle θ_{0i}, which serve as the generator of the tapping forces. This vehicle moves over a simply-supported bridge of length L at constant speed v. The bridge is modeled as a plane Bernoulli-Euler beam with bending stiffness EI and mass m per unit length. For simplicity but still keeping the essence of this problem, other practical factors, such as the damping and surface roughness etc., are temporarily ignored here. However, as was illustrated in the numerical examples in Section 3, the validity of the tap-scan method is not limited to this simple model.

2.1 Analytical formulation of the dynamic response

To obtain the vehicle dynamic response that is sensitive to bridge damage, one has to solve a vehicle-bridge interaction problem considering the tapping forces. According to the model depicted in Fig. 1, the kinematic equations of the vehicle and the bridge can be written as follows

$$M\,\ddot{y}_V + k(y_V - y_B|_{x=vt}) = F(t) \tag{1}$$

$$m\,\ddot{y}_B + EI\,y_B^{(\mathrm{IV})} = f(t)\,\delta(x - vt) \tag{2}$$

where y_V and y_B are the vehicle and bridge displacements measured from the static equilibrium

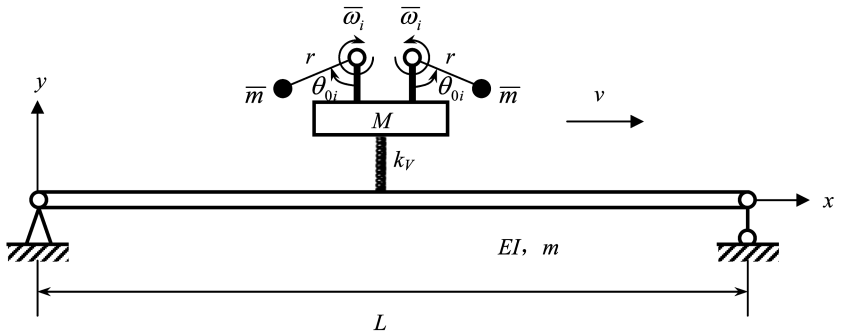

Fig. 1 A moving sprung mass with eccentric wheels

position, respectively. Here we ignore the bridge deflection induced by the gravity load of the vehicle mass, and assume that the bridge deflection induced by the bridge gravity load is compensated by the initial stress in the bridge girder, so that the static equilibrium position is always on the same level when the vehicle stands at different positions over the whole bridge deck. In addition, the symbol of double dots denotes the partial derivative over time t; $y_B^{(\mathrm{IV})} = \partial^4 y_B / \partial x^4$; and k is an effective stiffness which represents the series connection between the vehicle spring stiffness k_V and the bridge stiffness k_B

$$k = \frac{k_V k_B}{k_V + k_B} \tag{3}$$

The stiffness or spring constant k_B of the beam at the contact point can be evaluated as the ratio of a load acting at the contact point divided by the deflection generated at the same point. Using the fundamental theory of strength of materials, one can easily find that the deflection of an intact bridge under a unit load at position x is $(L-x)^2 x^2 / (3EIL)$. Thus, one can obtain the bridge stiffness k_B for the contact point $x = vt$ as

$$k_B = \frac{3EIL}{(L-x)^2 x^2} \tag{4}$$

Since k_B varies along the beam, the effective stiffness k also changes with position x.

The $F(t)$ in Eq. (1) is the tapping force applied on the vehicle

$$F(t) = -2\overline{m} r \sum_{i=1}^{N} \overline{\omega}_i^2 \cos(\overline{\omega}_i t + \theta_{0i}) \tag{5}$$

and $f(t)\delta(x - vt)$ is the contact force between the vehicle and bridge. Here, δ is the Kronecker delta function, which indicates the movement of the contact force. The function $f(t)$ can be expressed as

$$f(t) = k(y_V - y_B|_{x = vt}) - 2N\overline{m}g - Mg \tag{6}$$

For bridge structures, the mechanical damage can be defined as the abrupt change in stiffness or damping, which can be represented by the local impedance, or effectively the instantaneous stiffness $Z(x)$. From Eqs. (1), (2) and (6), one can write

$$Z(x) = \frac{f(t)}{y_B(t)} \delta(x - vt) = \frac{-M\ddot{y}_V\left(\frac{x}{v}\right) + F\left(\frac{x}{v}\right) - (2N\overline{m} + M)g}{y_B\left(\frac{x}{v}\right)} \tag{7}$$

which can be rewritten as

$$\ddot{y}_V(x) = -\frac{y_B\left(\frac{x}{v}\right)}{M} Z(x) + \frac{F\left(\frac{x}{v}\right)}{M} - \frac{2N\overline{m} + M}{M} g \tag{8}$$

Because the tapping force F and the vehicle mass $2N\overline{m} + M$ are constants, the value of y_B is

critical to the sensitivity of $\ddot{y}_V$ to damage. Using the modal superposition method, the bridge displacement can be expressed as

$$y_B(x,t) = \sum_{j=1}^{\infty} q_{Bj}(t)\varphi_j(x) \tag{9}$$

where $\varphi_j(x) = \sin\frac{j\pi x}{L}$ is the jth modal shape and $q_{Bj}(t)$ is the corresponding modal coordinate.

Substituting Eq. (9) into Eq. (2), multiplying $\varphi_j(x)$ on both sides and integrating over the bridge length, one obtains

$$\ddot{q}_{Bj} + \omega_{Bj}^2 q_{Bj} = \frac{2}{mL} f(x)\varphi_j(vt) \tag{10}$$

where ω_{Bj} is the jth natural angular frequency of the bridge

$$\omega_{Bj} = \left(\frac{j\pi}{L}\right)^2 \sqrt{\frac{EI}{m}} \tag{11}$$

Substituting Eqs. (1), (6) and $\varphi_j(x) = \sin\frac{j\pi x}{L}$ into Eq. (10) yields

$$\ddot{q}_{Bj} + \omega_{Bj}^2 q_{Bj} = -\frac{2}{mL}[M\ddot{y}_V - F(t) + 2N\overline{m}g + Mg]\sin\frac{j\pi vt}{L} \tag{12}$$

Generally $\ddot{y}_V << g$, otherwise one cannot ensure the firm contact between the vehicle and bridge. Therefore, Eq. (12) can be approximated as

$$\ddot{q}_{Bj} + \omega_{Bj}^2 q_{Bj} \approx -\frac{2}{mL}[-F(t) + (2N\overline{m} + M)g]\sin\frac{j\pi vt}{L} \tag{13}$$

With the use of Eq. (5), Eq. (13) can be solved by Duhamel's integral as follows

$$q_{Bj} = -\frac{2}{\omega_{Bj}mL}\int_0^t \left[2\overline{m}r\sum_{i=1}^{N}\overline{\omega}_i^2\cos(\overline{\omega}_i\tau + \theta_{0i}) + (2N\overline{m} + M)g\right]\sin\left(\frac{j\pi v\tau}{L}\right)\sin[\omega_{Bj}(t-\tau)]\,\mathrm{d}\tau$$

$$= \Delta_W\sum_{i=1}^{N}(R_j^i)^2\left\{S_j\left[\frac{\sin(\omega_{Bj}t + \theta_{0i})}{(R_j^i - 1)^2 - S_j^2} + \frac{\sin(\omega_{Bj}t - \theta_{0i})}{(R_j^i + 1)^2 - S_j^2}\right] + \frac{\sin\left[\left(\overline{\omega}_i + \frac{j\pi v}{L}\right)t + \theta_{0i}\right]}{(R_j^i + S_j)^2 - 1}\right.$$

$$\left. - \frac{\sin\left[\left(\overline{\omega}_i - \frac{j\pi v}{L}\right)t + \theta_{0i}\right]}{(R_j^i - S_j)^2 - 1}\right\} + \frac{\Delta_{Bj}}{1 - S_j^2}\left[\sin\left(\frac{j\pi v}{L}t\right) - S_j\sin(\omega_{Bj}t)\right] \tag{14}$$

where

$$\Delta_W = \frac{2\overline{m}r}{mL} \tag{15}$$

$$\Delta_{Bj} = -\frac{2(2N\overline{m}+M)gL^3}{(j\pi)^4 EI} \tag{16}$$

$$S_j = \frac{j\pi v}{L\omega_{Bj}} \tag{17}$$

$$R_j^i = \frac{\overline{\omega}_i}{\omega_{Bj}} \tag{18}$$

In Eq. (14), the initial velocity and displacement are ignored because they decay rapidly due to damping. Substituting Eq. (14) into Eq. (9), one obtains the bridge displacement as

$$y_B(x,t) = \Delta_W \sum_{j=1}^{\infty}\sum_{i=1}^{N} \sin\frac{j\pi x}{L}(R_j^i)^2 \left\{ S_j \left[\frac{\sin(\omega_{Bj}t+\theta_{0i})}{(R_j^i-1)^2-S_j^2} + \frac{\sin(\omega_{Bj}t-\theta_{0i})}{(R_j^i+1)^2-S_j^2} \right] + \frac{\sin\left[\left(\overline{\omega}_i+\frac{j\pi v}{L}\right)t+\theta_{0i}\right]}{(R_j^i+S_j)^2-1} - \frac{\sin\left[\left(\overline{\omega}_i-\frac{j\pi v}{L}\right)t+\theta_{0i}\right]}{(R_j^i-S_j)^2-1} \right\}$$

$$+ \sum_{j=1}^{\infty} \sin\frac{j\pi x}{L} \frac{\Delta_{Bj}}{1-S_j^2} \left[\sin\left(\frac{j\pi v}{L}t\right) - S_j \sin(\omega_{Bj}t) \right] \tag{19}$$

Further, substituting Eqs. (5) and (19) into Eq. (1) yields

$$\ddot{y}_V + \omega_V^2 y_V = G(t) \tag{20}$$

where ω_V is the natural angular frequency of the vehicle

$$\omega_V = \sqrt{\frac{k}{M}} \tag{21}$$

and

$$G(t) = \omega_V^2 \Delta_W \sum_{j=1}^{\infty}\sum_{i=1}^{N} \sin\left(\frac{j\pi v}{L}t\right)(R_j^i)^2 \left\{ S_j \left[\frac{\sin(\omega_{Bj}t+\theta_{0i})}{(R_j^i-1)^2-S_j^2} + \frac{\sin(\omega_{Bj}t-\theta_0)}{(R_j^i+1)^2-S_j^2} \right] + \frac{\sin\left[\left(\overline{\omega}_i+\frac{j\pi v}{L}\right)t+\theta_0\right]}{(R_j^i+S_j)^2-1} - \frac{\sin\left[\left(\overline{\omega}_i-\frac{j\pi v}{L}\right)t+\theta_0\right]}{(R_j^i-S_j)^2-1} \right\}$$

$$+ \omega_V^2 \sum_{j=1}^{\infty} \sin\left(\frac{j\pi v}{L}t\right) \frac{\Delta_{Bj}}{1-S_j^2} \left[\sin\left(\frac{j\pi v}{L}t\right) - S_j \sin(\omega_{Bj}t) \right] - \frac{2\overline{m}r}{M} \sum_{i=1}^{N} \overline{\omega}_i^2 \cos(\overline{\omega}_i t+\theta_0) \tag{22}$$

Similarly, by ignoring the initial displacement and velocity of the vehicle, the forced vibration of the vehicle can be solved from Eq. (20) by Duhamel's integral as

$$y_V = \frac{1}{\omega_V}\int_0^t G(\tau)\sin[\omega_V(t-\tau)]\mathrm{d}\tau$$

$$= \omega_V \sum_{j=1}^{\infty}\left[\sum_{i=1}^{N}\Delta_W (R_j^i)^2 P_j^i(t) + \frac{\Delta_{Bj}}{1-S_j^2}Q_j(t)\right]$$

$$-\frac{\overline{m}r}{M\omega_V}\sum_{i=1}^{N}\overline{\omega}_i^2\left[\frac{\cos(\omega_V t+\theta_{0i})}{\overline{\omega}_i-\omega_V} - \frac{\cos(\omega_V t-\theta_{0i})}{\overline{\omega}_i+\omega_V} - \frac{2\omega_V\cos(\overline{\omega}_i t+\theta_{0i})}{\overline{\omega}_i^2-\omega_V^2}\right] \tag{23}$$

where

$$P_j^i(t) = \frac{1}{2[(R_j^i+S_j)^2-1]}\left\{-\frac{\frac{j\pi v}{L}\cos(\omega_V t+\theta_{0i})}{\left(\frac{j\pi v}{L}\right)^2-\left(\overline{\omega}_i+\frac{j\pi v}{L}-\omega_V\right)^2} + \frac{\frac{j\pi v}{L}\cos(\omega_V t-\theta_{0i})}{\left(\frac{j\pi v}{L}\right)^2-\left(\overline{\omega}_i+\frac{j\pi V}{L}+\omega_V\right)^2}\right.$$

$$\left. + \omega_V\frac{\cos\left[\left(\frac{j2\pi v}{L}+\overline{\omega}_i\right)t+\theta_{0i}\right]}{\left(\frac{j2\pi v}{L}+\overline{\omega}_i\right)^2-\omega_v^2} - \omega_V\frac{\cos(\overline{\omega}_i t+\theta_{0i})}{\overline{\omega}_i^2-\omega_v^2}\right\}$$

$$-\frac{1}{2[(R_j^i-S_j)^2-1]}\left\{-\frac{\frac{j\pi v}{L}\cos(\omega_V t+\theta_{0i})}{\left(\frac{j\pi v}{L}\right)^2-\left(\overline{\omega}_i-\frac{j\pi v}{L}-\omega_V\right)^2} + \frac{\frac{j\pi v}{L}\cos(\omega_V t-\theta_{0i})}{\left(\frac{j\pi v}{L}\right)^2-\left(\overline{\omega}_i-\frac{j\pi v}{L}+\omega_V\right)^2}\right.$$

$$\left. + \omega_V\frac{\cos(\overline{\omega}_i t+\theta_{0i})}{\overline{\omega}_i^2-\omega_v^2} - \omega_V\frac{\cos\left[\left(\frac{j2\pi v}{L}-\overline{\omega}_i\right)t-\theta_{0i}\right]}{\left(\frac{j2\pi v}{L}-\overline{\omega}_i\right)^2-\omega_v^2}\right\}$$

$$+\frac{S_j}{2[(R_j^i-1)^2-S_j^2]}\left\{-\frac{\frac{j\pi v}{L}\cos(\omega_V t+\theta_{0i})}{\left(\frac{j\pi v}{L}\right)^2-(\omega_{Bj}-\omega_V)^2} + \frac{\frac{j\pi v}{L}\cos(\omega_V t-\theta_{0i})}{\left(\frac{j\pi v}{L}\right)^2-(\omega_{Bj}+\omega_V)^2}\right.$$

$$\left. + \omega_V\frac{\cos\left[\left(\frac{j\pi v}{L}+\omega_{Bj}\right)t+\theta_{0i}\right]}{\left(\frac{j\pi v}{L}+\omega_{Bj}\right)^2-\omega_V^2} - \omega_V\frac{\cos\left[\left(-\frac{j\pi v}{L}+\omega_{Bj}\right)t+\theta_{0i}\right]}{\left(\frac{j\pi v}{L}-\omega_{Bj}\right)^2-\omega_V^2}\right\}$$

$$-\frac{S_j}{2[(R_j^i+1)^2-S_j^2]}\left\{-\frac{\frac{j\pi v}{L}\cos(\omega_V t-\theta_{0i})}{\left(\frac{j\pi v}{L}\right)^2-(\omega_{Bj}-\omega_V)^2}+\frac{\frac{j\pi v}{L}\cos(\omega_V t+\theta_{0i})}{\left(\frac{j\pi v}{L}\right)^2-(\omega_{Bj}+\omega_V)^2}\right.$$

$$\left.+\omega_V\frac{\cos\left[\left(\frac{j\pi v}{L}+\omega_{Bj}\right)t-\theta_{0i}\right]}{\left(\frac{j\pi v}{L}+\omega_{Bj}\right)^2-\omega_V^2}-\omega_V\frac{\cos\left[\left(-\frac{j\pi v}{L}+\omega_{Bj}\right)t-\theta_{0i}\right]}{\left(\frac{j\pi v}{L}-\omega_{Bj}\right)^2-\omega_V^2}\right\} \tag{24}$$

$$Q_j(t)=\frac{\omega_V\cos\left(\frac{j2\pi v}{L}t\right)}{2\left[\left(\frac{j2\pi v}{L}\right)^2-\omega_V^2\right]}+\frac{1}{2\omega_V}-\frac{2\left(\frac{j\pi v}{L}\right)^2\cos(\omega_V t)}{\omega_V\left[\left(\frac{j2\pi v}{L}\right)^2-\omega_V^2\right]}$$

$$-S_j\omega_V\left\{\frac{\cos\left[\left(\frac{j\pi v}{L}+\omega_{Bj}\right)t\right]}{2\left[\left(\frac{j\pi v}{L}+\omega_{Bj}\right)^2-\omega_V^2\right]}-\frac{\cos\left[\left(\frac{j\pi v}{L}-\omega_{Bj}\right)t\right]}{2\left[\left(\frac{j\pi v}{L}-\omega_{Bj}\right)^2-\omega_V^2\right]}\right.$$

$$\left.+\frac{2\frac{j\pi v}{L}\omega_{Bj}\cos(\omega_V t)}{\left[\left(\frac{j\pi v}{L}+\omega_{Bj}\right)^2-\omega_V^2\right]\left[\left(\frac{j\pi v}{L}-\omega_{Bj}\right)^2-\omega_V^2\right]}\right\} \tag{25}$$

Consequently, the vehicle acceleration is

$$\ddot{y}_V=\omega_V\sum_{j=1}^{\infty}\left[\sum_{i=1}^{N}\Delta_W(R_j^i)^2\ddot{P}_j^i(t)+\frac{\Delta_{Bj}}{1-S_j^2}\ddot{Q}_j(t)\right]$$

$$+\frac{\overline{m}r}{M}\sum_{i=1}^{N}\overline{\omega}_i^2\left[\frac{\omega_V\cos(\omega_V t+\theta_{0i})}{\overline{\omega}_i-\omega_V}-\frac{\omega_V\cos(\omega_V t-\theta_{0i})}{\overline{\omega}_i+\omega_V}-\frac{2\overline{\omega}_i^2\cos(\overline{\omega}_i t+\theta_{0i})}{\overline{\omega}_i^2-\omega_V^2}\right] \tag{26}$$

where $\ddot{P}_j^i(t)$ and $\ddot{Q}_j(t)$ can be easily obtained from Eqs. (24) and (25), which are given in detail in Appendix.

2.2 Sensitivity analysis

According to the paper of Xiang and Zhang (2009), when local damage occurs, the global properties of the bridge do not change so much. That is to say, the bridge bending stiffness EI and the mass per unit length m do not change when a small damage is present. Consequently, the parameters ω_{Bj}, Δ_W, Δ_{Bj}, S_j and R_j^i in Eq. (26) do not change with a small damage. However, as

explained in Section 2.1, the bridge stiffness k_B varies over the span length of the bridge. A local damage can have great impact on k_B in its vicinity. Considering Eqs. (3) and (21), one may postulate that the vehicle frequency ω_V is sensitive to the damage. Therefore, the sensitivity of the vehicle acceleration can be evaluated as

$$\begin{aligned}\frac{\partial \ddot{y}_V}{\partial \omega_V} &= \sum_{j=1}^{\infty}\left[\sum_{i=1}^{N}\Delta_W (R_j^i)^2 \ddot{P}_j^i + \frac{\Delta_{Bj}}{1-S_j^2}\ddot{Q}_j\right] + \omega_V \sum_{j=1}^{\infty}\left[\sum_{i=1}^{N}\Delta_W (R_j^i)^2 \frac{\partial \ddot{P}_j^i}{\partial \omega_V} + \frac{\Delta_{Bj}}{1-S_j^2}\frac{\partial \ddot{Q}_j}{\partial \omega_V}\right] \\ &+ \frac{\overline{m}r}{M}\sum_{i=1}^{N}\overline{\omega}_i^2\left[\frac{\cos(\omega_V t+\theta_{0i})}{\overline{\omega}_i-\omega_V} - \frac{\omega_V \sin(\omega_V t+\theta_{0i})t}{\overline{\omega}_i-\omega_V} + \frac{\omega_V \cos(\omega_V t+\theta_{0i})}{(\overline{\omega}_i-\omega_V)^2}\right. \\ &\left. - \frac{\cos(\omega_V t-\theta_{0i})}{\overline{\omega}_i+\omega_V} + \frac{\omega_V \sin(\omega_V t-\theta_{0i})t}{\overline{\omega}_i+\omega_V} + \frac{\omega_V \cos(\omega_V t-\theta_{0i})}{(\overline{\omega}_i+\omega_V)^2} - \frac{4\omega_V \overline{\omega}_i^2 \cos(\overline{\omega}_i^t+\theta_{0i})}{(\overline{\omega}_i^2-\omega_V^2)^2}\right]\end{aligned} \tag{27}$$

where $\partial \ddot{P}_j^i / \partial \omega_V$ and $\partial \ddot{Q}_j / \partial \omega_V$ can be easily obtained from Eqs. (A1) and (A2), respectively.

From Eqs. (26), (27) and Eqs. (15) through (18), one observes that various approaches exist for enhancing the sensitivity of vehicle acceleration to damage, as listed below:

(1) Increase Δ_W, Δ_{Bj} and $\overline{m}r\overline{\omega}_i^2/M$, i.e., using a light vehicle and heavy tapping force. However, the condition of $\ddot{y}_V << g$ should always be satisfied to ensure the firm contact between the vehicle and bridge.

(2) Let the tapping frequency $\overline{\omega}_i$ be close to ω_V, and avoid the resonance of the vehicle, but still ensure $\ddot{y}_V << g$.

(3) $S_j \approx 1$. According to Eq. (17), this means a very high vehicle speed, which can hardly happen in practice. Usually, $S_j << 1$.

(4) $R_j^i \approx 1 \pm S_j$, i.e., $\overline{\omega}_i \approx \omega_{Bj} \pm (j\pi v/L)$. This means that it is better to let the tapping frequency be close to the bridge natural frequency. However, according to Eq. (19), one should pay attention to avoiding the resonance of the bridge.

(5) $\omega_V \approx \omega_{Bj} \pm (j\pi v/L)$. This means the vehicle stiffness can be carefully adjusted for a specific bridge and a moving velocity v, so that the vehicle acceleration is sensitive to damage, while avoiding the resonance of the vehicle.

(6) $\omega_V \approx (j2\pi v/L)$. This can hardly happen in practice (Yang *et al.* 2004).

2.3 Damage identification method

Generally, the damage identification can be investigated under the framework of statistic pattern recognition, which contains mainly four key steps: operational evaluation, data acquisition, feature selection and feature discrimination (Farrar and Worden 2007).

For the tap-scan method proposed in this paper, the operational evaluation results in the scheme of using a moving vehicle mounted with a tapping device to scan the damage information of a bridge. Here damage is regarded as the change of local impedance, which is contained in the vehicle acceleration. This can be proved by simply transfer Eq. (26) into frequency domain, by which seven kinds of frequencies can be observed from the spectrum, i.e., ω_V, $\overline{\omega}_i$, $\overline{\omega}_i + (j2\pi v/L)$, $\overline{\omega}_i - (j2\pi v/L)$, $\omega_{Bj} + (j\pi v/L)$, $\omega_{Bj} - (j\pi v/L)$ and $j2\pi v/L$. Because $j\pi v/L$ is usually very

small, only ω_V, $\bar{\omega}_i$ and ω_{Bj} are dominant. As was explained in Section 2.2, the damage, i.e., the change of ω_V, can change the coefficient of the terms corresponding to each frequency in Eq. (26). As such, the spectrum contour of the vehicle acceleration is expected to contain the damage information.

According to the above discussion, the spectrum contour of the vehicle acceleration is selected as the damage feature. In practical implementation, the signal of vehicle acceleration is uniformly subdivided into n segments. In each segment, the acceleration signal is regarded as stationary, so that the Short Time Fourier Transformation (STFT) can be applied to obtain the power spectrum of each segment. The amplitude at frequencies of ω_V, $\bar{\omega}_i$ and ω_{Bj} are recorded into a feature vector $\boldsymbol{Y}$, which contains information of the effective damage in that segment. The MAC index proposed by Allemang and Brown (1982) can be used to discriminate two feature vectors $\boldsymbol{Y}_i$ and $\boldsymbol{Y}_j$ ($i, j = 1, 2, \ldots, n$)

$$MAC(i,j) = \frac{\boldsymbol{Y}_i \bullet \boldsymbol{Y}_j}{\|\boldsymbol{Y}_i\|\|\boldsymbol{Y}_j\|} \qquad i, j = 1, 2, \ldots, n \tag{28}$$

It is noticed that the MAC value equals one if two feature vectors are identical and the smaller the MAC value, the larger difference between these two vectors. If one plots the surface of the MAC matrix obtained from Eq. (28), an abrupt change in value can indicate the existence of a damage, because the local impedance usually changes smoothly over an intact structure. This means that the *finger-print* of intact structure is not necessary. In other words, no supervised learning is required of the tap-scan method, which should greatly facilitate its practical implementation.

3. Numerical examples

In this section, numerical examples are presented to firstly check the validity of the theoretical formulation presented in Section 2 and then to illustrate the potential of the proposed tap-scan method. All the vehicle-bridge interaction problems are simulated by the ABAQUS implicit Finite Element (FE) package with time step of 0.001s.

3.1 Verification of the analytic solution of vehicle acceleration

To evaluate the validity of the analytical solution of the vehicle acceleration presented in Section 2.1, the example of a simply-supported beam without damage is adopted from the paper of Yang *et al*. (2004). The properties of the beam are: cross-sectional area $A = 2.0\ \mathrm{m}^2$, moment of inertia $I = 0.12\ \mathrm{m}^4$, length $L = 25$ m, elastic modulus $E = 27.5\ \mathrm{GN/m}^2$, and mass per unit length $m = 4800$ kg/m. A vehicle with a mass of $M = 1200$ kg, spring stiffness of $k_V = 500$ kN/m and zero damping passes through the bridge at a constant speed $v = 10$ m/s. In the following simulation, the beam is modeled by 2-node plane beam elements with a length of 0.2 m.

In the first simulation, no tapping force is applied on the vehicle, as a degenerated case of the tap-scan problem. The analytical vehicle acceleration is compared with the numerical result in Fig. 2(a), which reveals that the analytical result is in good agreement with the numerical one, and naturally the same as that of Yang *et al*. (2004).

In the second simulation, an external tapping force is applied. The tapping device is equivalent to an eccentric wheel with mass $\bar{m} = 10\mathrm{kg}$ and arm length $r = 1\mathrm{m}$, which rotates at $\bar{\omega} = 10\mathrm{rad/s}$

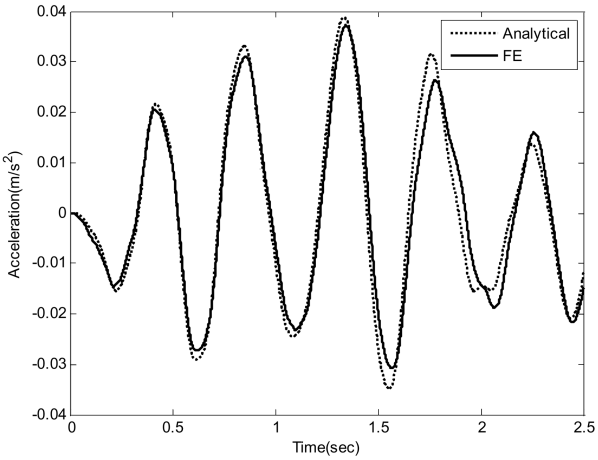

(a) Without tapping load

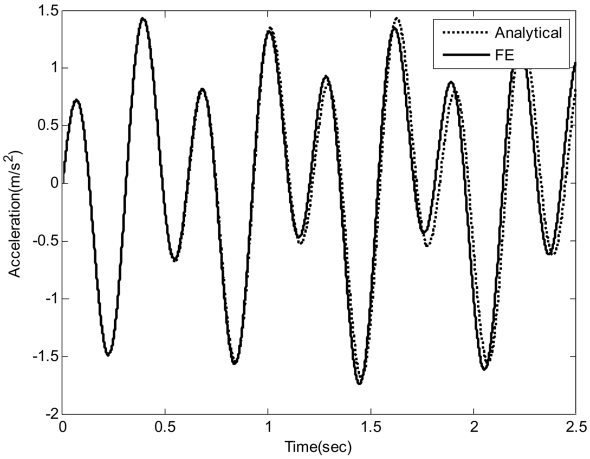

(b) With tapping load

Fig. 2 The acceleration of vehicle that moves on an intact simply-supported beam: (a) Without tapping load, (b) With tapping load

with an initial angle $\theta_0 = \pi/2$. As shown in Fig. 2(b), the analytical vehicle acceleration agrees very well with the numerical result. Although, only one pair of eccentric masses is introduced here for simplicity, this example can still prove the validity of the analytical results presented in Section 2.1.

3.2 Damage identification of a smooth simply-supported beam without damage

In this section, a vehicle with a mass of $M = 1200$ kg, spring stiffness of $k_V = 5000$ kN/m and 5% damping is adopted to scan the same intact bridge in Section 3.1 at a constant speed $v = 1$ m/s. It is

interesting to check what will happen if the damage identification is conducted for this intact bridge. Following the tap-scan method proposed in Section 2.2, the time series of vehicle acceleration is subdivided into 25 segments, i.e., one second or one meter per segment. Then, the STFT method is used to generate the power spectrum for each segment. The contour of each power spectrum is compared with each other to get the MAC matrix based on Eq. (28), from which one can observe the damage information.

In the first simulation, no tapping force is applied. From the power spectrum (a typical one is shown in Fig. 3), one can identify three peaks corresponding to $\omega_{B1} \pm (\pi v / L)$ (about 2.06 Hz), $\omega_{B2} \pm (2\pi v / L)$ (about 8.24 Hz), and vehicle frequency ω_V (10.27 Hz). Recording the amplitudes from 1 to 11 Hz with 1 Hz interval, one obtains the damage feature vector $\boldsymbol{Y}_i$ (i = 1, 2, …, 25). Then, the MAC matrix can be calculated by Eq. (28) (as plotted in Fig. 4). As can be seen, the MAC values are almost the same over the bridge span, which shows no sign of damage.

In the second simulation, the vehicle is mounted with four pairs of eccentric wheels with mass $\overline{m}$ = 0.5 kg and arm length r = 1m, rotating at the frequencies of $\overline{\omega}$ = (1.00 2.50 4.00 5.50) × 2π(rad/s) with an initial angle $\theta_0 = \pi/2$. From the power spectrum (a typical one is shown in Fig. 5), one can identify four peaks corresponding to $\overline{\omega}_2$ (2.5 Hz), $\overline{\omega}_3$ (4.00 Hz), $\overline{\omega}_4$ (5.5 Hz) and vehicle frequency ω_V (10.27 Hz). Recording the amplitudes from 1 to 11 Hz with 1 Hz interval, one obtains the damage feature vector $\boldsymbol{Yi}$ (i = 1, 2, …, 25). Then, the MAC matrix can be calculated by using Eq. (28) (as plotted in Fig. 6). As can be observed from the two edges of the MAC matrix surface, the MAC value changes smoothly over the beam span following a similar curve of $(L-x)^2x^2/(3EIL)$. This represents the change of the beam stiffness (referring to Eq. (4)) and indicates the absence of damage. Comparing Figs. 4 with 6, one finds out that the change of beam stiffness can hardly be identified without the tapping load.

3.3 Damage identification of a smooth simply-supported beam with a midspan damage

Taking the similar example of Section 3.2, but assuming the 50 cm segment in the middle of the

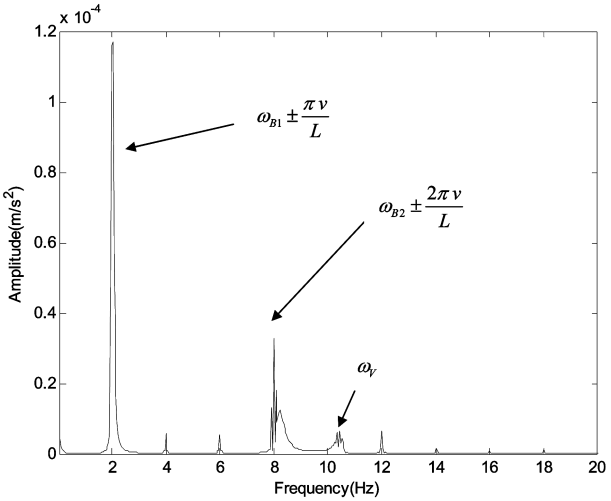

Fig. 3 Power spectrum of the middle segment of the intact beam (without tap)

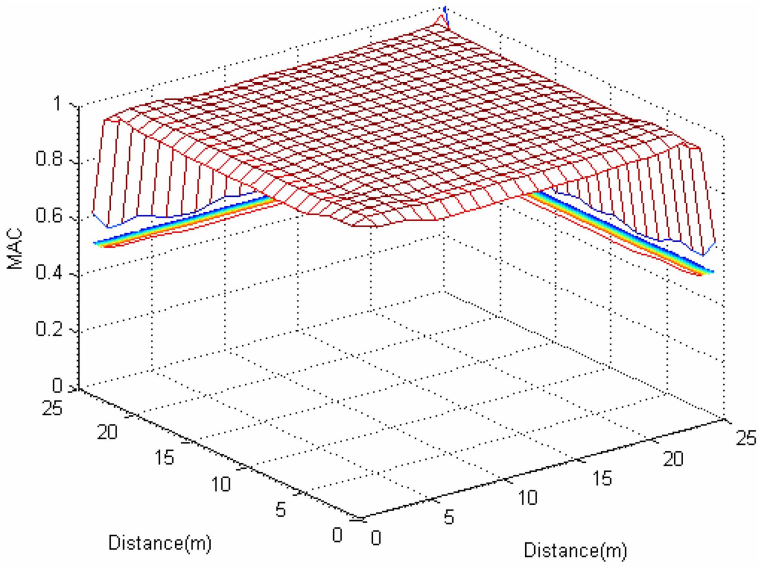

Fig. 4 Damage identification results of the intact simply-supported beam (without tap)

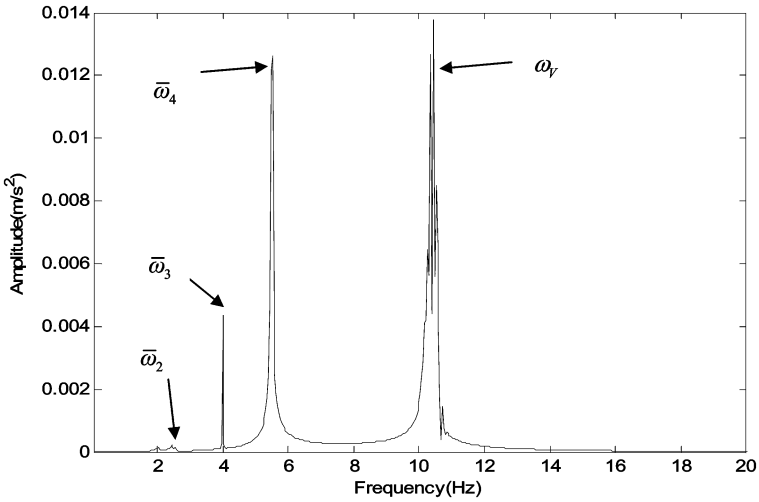

Fig. 5 Power spectrum of the middle segment of the intact beam (with tap)

smooth beam to be damaged, we shall examine the damage identification ability of the tap-scan method.

In the first simulation, the bending stiffness of the damaged region is reduced by 10 % and no tapping force is applied to the vehicle. Fig. 7(a) shows the MAC matrix for this case, from which the damage can hardly be identified. This implies that it is generally hard to identify the damage without the tapping force. This verifies the approach (1) discussed in Section 2.2.

In the second simulation, a 10 % reduction in bending stiffness of the damaged region is assumed and the tapping forces at frequencies of $\bar{\omega} = (1.00 \;\; 2.50 \;\; 4.00 \;\; 5.50) \times 2\pi(\mathrm{rad/s})$ are applied to the vehicle. From the MAC matrix plotted in Fig. 7(b), one observes that no damage can be

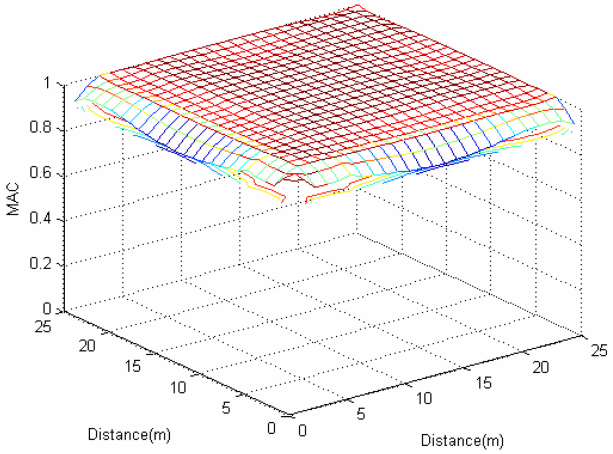

Fig. 6 Damage identification results of the intact simply-supported beam (with tap)

identified, due to the fact that the tapping frequency is neither close to ω_{Bj} nor to ω_V.

In the third simulation, a 10% reduction in bending stiffness of the damaged region is assumed and the tapping forces of frequencies $\bar{\omega} = (1.00 \quad 4.00 \quad 5.50 \quad 10.50) \times 2\pi(\mathrm{rad/s})$ are applied to the vehicle. As shown in Fig. 7(c), the vehicle acceleration appears to be much greater than 9.8 m/s^2, an evidence of the resonant phenomenon. Referring to the approach (2) in Section 2.2, i.e., we conclude that it can be very dangerous to set one tapping frequency close to the vehicle frequency ω_V.

In the fourth simulation, the bending stiffness is reduced by 10% in the damaged region and the tapping forces at frequencies of $\bar{\omega} = (2.00 \quad 3.30 \quad 8.40 \quad 18.50) \times 2\pi(\mathrm{rad/s})$ are applied to the vehicle. As revealed by Fig. 7(d), there is an abrupt change in the corresponding MAC matrix, which indicates the correct location of damage. This verifies the approach (4) in Section 2.2, by setting the tapping frequencies close to the bridge frequency ω_{Bj}.

The case of the fifth simulation is almost the same as that in the second simulation, except for reduction of the vehicle frequency to $\omega_V = 2.10 \times 2\pi(\mathrm{rad/s})$. The corresponding vehicle acceleration has been plotted in Fig. 7(e), which implies the occurrence of resonance. With reference to the approach (5) in Section 2.2, which recommends adjusting ω_V close to ω_{Bj}, the conclusion is that this cannot be so easy in practice and has the risk of producing resonance.

The case of the sixth simulation is almost the same as that in the fourth simulation, except for the 5% reduction in bending stiffness at the damaged region. It is interesting to compare the corresponding MAC matrix shown in Fig. 7(f) with the one in Fig. 7(d). One observes that although the damage can be identified in both cases, the smaller damage produces the smaller drop in the MAC value. This indicates that damage severity can be justified from the drop of the MAC value.

3.4 Damage identification of a rough simply-supported beam with a midspan damage

This section is aimed at examining the tap-scan method in a noisy environment. Here we consider the roughness of the surface of bridge deck, which adds some white noise into the vehicle acceleration. Following the paper of Bu *et al.* (2006), the polluted vehicle acceleration $\ddot{y}_{Vp}$ can be calculated as follows

$$\ddot{y}_{Vp} = \ddot{y}_V + E_p \cdot N_{oise} \cdot \sigma(\ddot{y}_V) \tag{29}$$

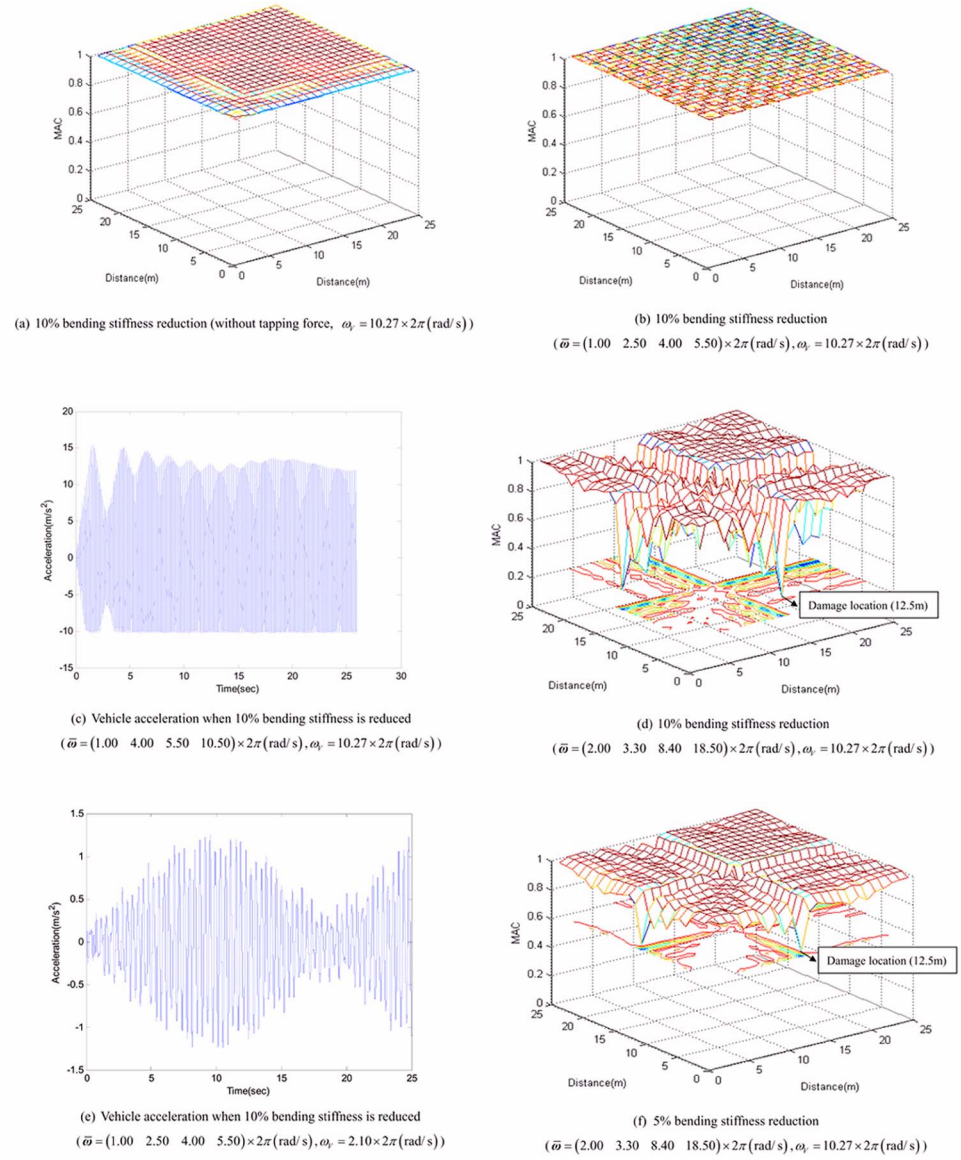

(a) 10% bending stiffness reduction (without tapping force, $\omega_V = 10.27 \times 2\pi\,(\mathrm{rad/s})$)

(b) 10% bending stiffness reduction ($\overline{\boldsymbol{\omega}} = (1.00 \;\; 2.50 \;\; 4.00 \;\; 5.50) \times 2\pi(\mathrm{rad/s})$, $\omega_V = 10.27 \times 2\pi\,(\mathrm{rad/s})$)

(c) Vehicle acceleration when 10% bending stiffness is reduced ($\overline{\boldsymbol{\omega}} = (1.00 \;\; 4.00 \;\; 5.50 \;\; 10.50) \times 2\pi(\mathrm{rad/s})$, $\omega_V = 10.27 \times 2\pi\,(\mathrm{rad/s})$)

(d) 10% bending stiffness reduction ($\overline{\boldsymbol{\omega}} = (2.00 \;\; 3.30 \;\; 8.40 \;\; 18.50) \times 2\pi(\mathrm{rad/s})$, $\omega_V = 10.27 \times 2\pi\,(\mathrm{rad/s})$)

(e) Vehicle acceleration when 10% bending stiffness is reduced ($\overline{\boldsymbol{\omega}} = (1.00 \;\; 2.50 \;\; 4.00 \;\; 5.50) \times 2\pi(\mathrm{rad/s})$, $\omega_V = 2.10 \times 2\pi\,(\mathrm{rad/s})$)

(f) 5% bending stiffness reduction ($\overline{\boldsymbol{\omega}} = (2.00 \;\; 3.30 \;\; 8.40 \;\; 18.50) \times 2\pi(\mathrm{rad/s})$, $\omega_V = 10.27 \times 2\pi\,(\mathrm{rad/s})$)

Fig. 7 Damage identification results of the simply-supported smooth beam damaged in the middle
(a) 10% bending stiffness reduction (without tapping force, $\omega_V = 10.27 \times 2\pi\,(\mathrm{rad/s})$)
(b) 10% bending stiffness reduction ($\overline{\boldsymbol{\omega}} = (1.00 \;\; 2.50 \;\; 4.00 \;\; 5.50) \times 2\pi(\mathrm{rad/s})$, $\omega_V = 10.27 \times 2\pi\,(\mathrm{rad/s})$)
(c) Vehicle acceleration when 10% bending stiffness is reduced ($\overline{\boldsymbol{\omega}} = (1.00 \;\; 4.00 \;\; 5.50 \;\; 10.50) \times 2\pi(\mathrm{rad/s})$, $\omega_V = 10.27 \times 2\pi\,(\mathrm{rad/s})$)
(d) 10% bending stiffness reduction ($\overline{\boldsymbol{\omega}} = (2.00 \;\; 3.30 \;\; 8.40 \;\; 18.50) \times 2\pi(\mathrm{rad/s})$, $\omega_V = 10.27 \times 2\pi\,(\mathrm{rad/s})$)
(e) Vehicle acceleration when 10% bending stiffness is reduced ($\overline{\boldsymbol{\omega}} = (1.00 \;\; 2.50 \;\; 4.00 \;\; 5.50) \times 2\pi(\mathrm{rad/s})$, $\omega_V = 2.10 \times 2\pi\,(\mathrm{rad/s})$)
(f) 5% bending stiffness reduction ($\overline{\boldsymbol{\omega}} = (2.00 \;\; 3.30 \;\; 8.40 \;\; 18.50) \times 2\pi(\mathrm{rad/s})$, $\omega_V = 10.27 \times 2\pi\,(\mathrm{rad/s})$)

where $\ddot{y}_V$ is the clean vehicle acceleration from the finite element simulation; E_p is the noise level; N_{oise} is the standard normal distribution with zero mean and unit standard deviation; and $\sigma(\ddot{y}_V)$ is

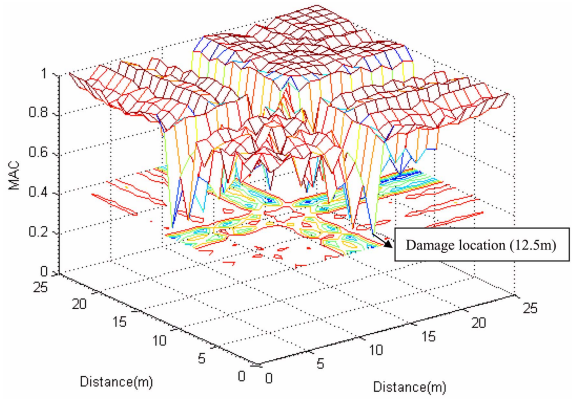

(a) 10% noise level

($\bar{\omega} = (2.00 \quad 3.30 \quad 8.40 \quad 18.50) \times 2\pi\,(\text{rad/s}), \omega_V = 10.27 \times 2\pi\,(\text{rad/s})$)

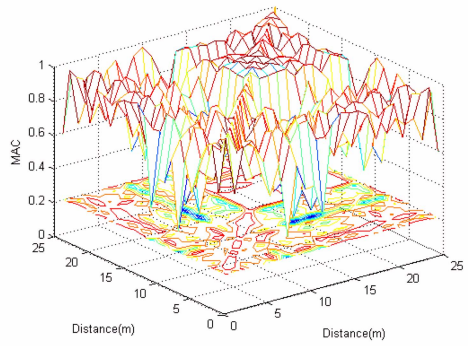

(b) 30% noise level

($\bar{\omega} = (2.00 \quad 3.30 \quad 8.40 \quad 18.50) \times 2\pi\,(\text{rad/s}), \omega_V = 10.27 \times 2\pi\,(\text{rad/s})$)

Fig. 8 Damage identification results of the simply-supported rough beam with 5% bending stiffness reduction in the middle
10% noise level ($\bar{\omega} = (2.00 \quad 3.30 \quad 8.40 \quad 18.50) \times 2\pi(\text{rad/s})$, $\omega_V = 10.27 \times 2\pi\,(\text{rad/s})$)
30% noise level ($\bar{\omega} = (2.00 \quad 3.30 \quad 8.40 \quad 18.50) \times 2\pi(\text{rad/s})$, $\omega_V = 10.27 \times 2\pi\,(\text{rad/s})$)

the standard deviation of $\ddot{y}_V$.

In this simulation, the value $\ddot{y}_V$ in Eq. (29) is just taken as the vehicle acceleration of the fourth case in Section 3.2. Figs. 8(a) and 9(b) show the damage identification results with the noise level of 10% and 30%, respectively. A comparison of these figures with Fig. 7(d) indicates that the more severe of the noise interference is, the weaker the probability for damage identification. However, because the tapping frequency is specially tuned to enhance the sensitivity, the small damage in bending stiffness can still be identified even in a noisy environment.

4. Conclusions

Combining the passing vehicle method of Yang *et al.* (2004) with the tap test method, this paper

proposes a tap-scan method for the damage detection of bridge structures. The closed form solution of the theoretical model of this problem is obtained analytically. Based on that, the sensitivity of the vehicle acceleration to damage is discussed in detail. It is confirmed that the spectrum contour of the vehicle acceleration contains the damage information.

The tap-scan method is constructed under the framework of statistic pattern recognition. All the theoretical bases are verified by the numerical examples. It is concluded that the tap-scan method is effective when the tapping load frequency is tuned to be close to the bridge natural frequencies. The tap-scan method has the potential of providing an economical approach to detect damages in bridge structures without the requirement of mounting sensors on the bridge or blocking the ongoing bridge traffic. However, further works are necessary for experimental verification, while examining the applicability of this method to different damage scenarios for different types of bridges.

Acknowledgements

This work is support by National Science Foundation of China with grant number 10802040). Such a financial support is gratefully acknowledged.

References

Allemang, R.J. and Brown, D.L. (1982), "Correlation coefficient for modal vector analysis", *Proceedings of the 1st International Modal Analysis Conference*, Society for Experimental Mechanics, Orlando, 110-116.

Bu, J.Q., Law, S.S. and Zhu, X.Q. (2006), "Innovative bridge condition assessment from dynamic response of a passing vehicle", *J. Eng. Mech.*, **132**, 1372-1378.

Carden, E.P. and Fanning, P. (2004), "Vibration based condition monitoring: a review", *Struct. Health Monitor.*, **3**, 355-377.

Cawley, P. and Adams, R.D. (1988), "The mechanics of the coin-tap method of non-destructive testing", *J. Sound Vib.*, **122**, 299-316.

Cawley, P. and Adams, R.D. (1989), "Sensitivity of the coin-tap method of non-destructive testing", *Mater. Eval.*, **122**, 299-316.

Farrar, C.R., Doebling, S.W. and Nix, D.A. (2001), "Vibration-based structural damage identification", *Philos. T. R. Soc. A*, **359**, 131-149.

Farrar, C.R. and Worden, K. (2007), "An introduction to structural health monitoring", *Philos. T. R. Soc. A*, **365**, 303-315.

Lin, C.W. and Yang, Y.B. (2005), "Use of a passing vehicle to scan the fundamental bridge frequencies", *Eng. Struct.*, **27**, 1865-1878.

Majumder, L. and Manohar, C.S. (2003), "A time-domain approach for damage detection in beam structures using vibration data with a moving oscillator as an excitation source", *J. Sound Vib.*, **268**, 699-716.

Majumder, L. and Manohar, C.S. (2004), "Nonlinear reduced models for beam damage detection using data on moving oscillator-beam interactions", *Comput. Struct.*, **82**, 301-314.

Xiang, Z.H. and Zhang, Y. (2009), "Change of modal properties of simply-supported plane beams due to damages", *Interact. Multiscale Mech.*, **2**, 153-175.

Yang, Y.B., Lin, C.W. and Yau, J.D. (2004), "Extracting bridge frequencies from the dynamic response of a passing vehicle", *J. Sound Vib.*, **272**, 471-493.

Yang, Y.B. and Chang, K.C. (2009), "Extraction of bridge frequencies from the dynamic response of a passing vehicle enhanced by the EMD technique", *J. Sound Vib.*, **322**, 718-739.

Yang, Y.B. and Chang, K.C. (2009), "Extracting the bridge frequencies indirectly from a passing vehicle: Parametric study", *Eng. Struct.*, **31**, 2448-2459.

Appendix

The terms $\ddot{P}_j(t)$ and $\ddot{Q}_j(t)$ in Eq. (26) are derived as follows:

$$\begin{aligned}
\ddot{P}_j^i(t) = & \frac{1}{2[(R_j^i+S_j)^2-1]}\left\{\frac{\frac{j\pi v}{L}\omega_V^2\cos(\omega_V t+\theta_{0i})}{\left(\frac{j\pi v}{L}\right)^2-\left(\overline{\omega}_i+\frac{j\pi v}{L}-\omega_V\right)^2}-\frac{\frac{j\pi v}{L}\omega_V^2\cos(\omega_V t-\theta_{0i})}{\left(\frac{j\pi v}{L}\right)^2-\left(\overline{\omega}_i+\frac{j\pi v}{L}+\omega_V\right)^2}\right. \\
& \left.-\omega_V\left(2\frac{j\pi v}{L}+\overline{\omega}_i\right)^2\frac{\cos\left[\left(2\frac{j\pi v}{L}+\overline{\omega}_i\right)t+\theta_{0i}\right]}{\left(2\frac{j\pi v}{L}+\overline{\omega}_i\right)^2-\omega_V^2}+\omega_V\overline{\omega}_i^2\frac{\cos(\overline{\omega}_i t+\theta_{0i})}{\overline{\omega}_i^2-\omega_v^2}\right\} \\
& -\frac{1}{2[(R_j^i-S_j)^2-1]}\left\{\frac{\frac{j\pi v}{L}\omega_V^2\cos(\omega_V t+\theta_{0i})}{\left(\frac{j\pi v}{L}\right)^2-\left(\overline{\omega}_i-\frac{j\pi v}{L}-\omega_V\right)^2}-\frac{\frac{j\pi v}{L}\omega_V^2\cos(\omega_V t-\theta_{0i})}{\left(\frac{j\pi v}{L}\right)^2-\left(\overline{\omega}_i-\frac{j\pi v}{L}+\omega_V\right)^2}\right. \\
& \left.+\omega_V\left(2\frac{j\pi v}{L}-\overline{\omega}_i\right)^2\frac{\cos\left[\left(2\frac{j\pi v}{L}-\overline{\omega}_i\right)t-\theta_{0i}\right]}{\left(\frac{j\pi 2 v}{L}-\overline{\omega}_i\right)^2-\omega_V^2}-\omega_V\overline{\omega}_i^2\frac{\cos(\overline{\omega}_i t+\theta_{0i})}{\overline{\omega}_i^2-\omega_V^2}\right\} \\
& +\frac{S_j}{2[(R_j^i-1)^2-S_j^2]}\left\{\frac{\frac{j\pi v}{L}\omega_V^2\cos(\omega_V t+\theta_{0i})}{\left(\frac{j\pi v}{L}\right)^2-(\omega_{Bj}-\omega_V)^2}-\frac{\frac{j\pi v}{L}\omega_V^2\cos(\omega_V t-\theta_{0i})}{\left(\frac{j\pi v}{L}\right)^2-(\omega_{Bj}+\omega_V)^2}\right. \\
& \left.-\omega_V\left(\frac{j\pi v}{L}+\omega_{Bj}\right)^2\frac{\cos\left[\left(\frac{j\pi v}{L}+\omega_{Bj}\right)t+\theta_{0i}\right]}{\left(\frac{j\pi v}{L}+\omega_{Bj}\right)^2-\omega_V^2}+\omega_V\left(\frac{j\pi v}{L}+\omega_{Bj}\right)^2\frac{\cos\left[\left(-\frac{j\pi v}{L}+\omega_{Bj}\right)t+\theta_{0i}\right]}{\left(\frac{j\pi v}{L}-\omega_{Bj}\right)^2-\omega_V^2}\right\} \\
& -\frac{S_j}{2[(R_j^i+1)^2-S_j^2]}\left\{\frac{\frac{j\pi v}{L}\omega_V^2\cos(\omega_V t+\theta_{0i})}{\left(\frac{j\pi v}{L}\right)^2-(\omega_{Bj}-\omega_V)^2}-\frac{\frac{j\pi v}{L}\omega_V^2\cos(\omega_V t+\theta_{0i})}{\left(\frac{j\pi v}{L}\right)^2-(\omega_{Bj}+\omega_V)^2}\right. \\
& \left.-\omega_V\left(\frac{j\pi v}{L}+\omega_{Bj}\right)^2\frac{\cos\left[\left(\frac{j\pi v}{L}+\omega_{Bj}\right)t-\theta_{0i}\right]}{\left(\frac{j\pi v}{L}+\omega_{Bj}\right)^2-\omega_V^2}+\omega_V\left(-\frac{j\pi v}{L}+\omega_{Bj}\right)^2\frac{\cos\left[\left(-\frac{j\pi v}{L}+\omega_{Bj}\right)t-\theta_{0i}\right]}{\left(\frac{j\pi v}{L}-\omega_{Bj}\right)^2-\omega_V^2}\right\} \quad \text{(A1)}
\end{aligned}$$

$$\ddot{Q}_j(t) = \frac{2\omega_V\left[\frac{j\pi v}{L}\right]^2\left[\cos(\omega_V t) - \cos\left(\frac{j2\pi v}{L}t\right)\right]}{\left(\frac{j2\pi v}{L}\right)^2 - \omega_V^2}$$

$$-S_j\omega_V\left\{-\left(\frac{j\pi v}{L} + \omega_{Bj}\right)^2 \frac{\cos\left[\left(\frac{j\pi v}{L} + \omega_{Bj}\right)t\right]}{2\left[\left(\frac{j\pi v}{L} + \omega_{Bj}\right)^2 - \omega_V^2\right]} + \left(\frac{j\pi v}{L} - \omega_{Bj}\right)^2 \frac{\cos\left[\left(\frac{j\pi v}{L} - \omega_{Bj}\right)t\right]}{2\left[\left(\frac{j\pi v}{L} - \omega_{Bj}\right)^2 - \omega_V^2\right]}\right.$$

$$\left. - \frac{2\frac{j\pi v}{L}\omega_{Bj}\omega_V^2\cos(\omega_V t)}{\left[\left(\frac{j\pi v}{L} + \omega_{Bj}\right)^2 - \omega_V^2\right]\left[\left(\frac{j\pi v}{L} - \omega_{Bj}\right)^2 - \omega_V^2\right]}\right\} \tag{A2}$$